

Carbon nanostructures/cadmium-sulfide hybrid heterostructures formation

A. Cortes · E. Svåsand · V. Lavayen ·
R. Segura · P. Häberle

Received: 30 October 2009 / Accepted: 24 February 2010 / Published online: 12 March 2010
© Springer Science+Business Media, LLC 2010

Abstract We present a simple method for preparing heterostructures based on cadmium sulfide thin films modified by the addition of carbon nanostructures. For this particular system, we have examined the effect on the photocurrent produced by the addition of multiwall carbon nanotubes or multiwall carbon nanocones between the transparent metallic electrode and CdS, a II–VI semiconductor. Our preliminary results indicate the photocurrent through the semiconductor is strongly modified by the presence of carbon nanotubes or carbon cones.

Introduction

Assembling multifunctional nanostructures with two or more types of materials, using covalent or noncovalent approaches, can add or extend new functionalities of these structures and opens the possibility of novel applications. The combination of cadmium sulfide (CdS) and carbon nanostructures is one such hybrid material. CdS is a direct bandgap semiconductor (gap 2.42 [1]), and has many applications, for instance in light detection. Thin films of CdS are required in components such as photoresistors and photovoltaic (PV) cells. In PV cells, CdS forms a heterojunction with cadmium telluride (CdTe), which is the

absorbing layer. A current problem in CdS/CdTe PV cells is finding ways to facilitate the transport of electrons/holes to the circuit before the recombination process occurs. Using carbon nanostructures in combination with one of the semiconductor layers has proven useful in increasing the charge collection efficiency of the heterostructure thin films, as measured by the photocurrent output. Willner and coworkers coupled carbon nanotubes (CNTs) to a gold substrate and then deposited CdS particles on top. This combination showed enhanced photocurrent as opposed to CdS alone [2]. Similar results were reported by Kamat and coworkers. They have deposited single-wall carbon nanotubes (SWCNTs) films using electrophoresis and then modified the layer with CdS particles [3]. Lee and coworkers decorated SWCNT with CdS nanocrystals (NC) dropping a solution of NC onto a positively charged SWCNT-field effect transistor (FET). This technique immobilized the NC on the SWCNTs [4].

In the present paper, we report a simple and scalable method for creating hybrid heterostructure CdS/carbon nanostructures. The optical properties of these films have been investigated. The presence of MWCNTs or MWCNCs strongly modifies the photoconductivity of the films. The physical interpretation of the results is discussed.

Experimental procedure

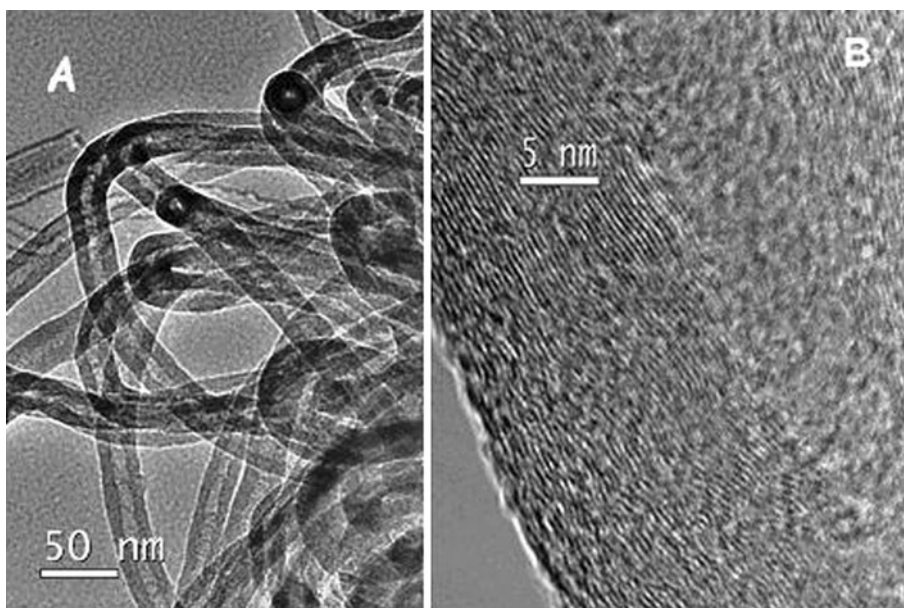
Carbon nanomaterials

Multiwall carbon nanotubes (MWCNTs) were synthesized by thermal chemical vapor deposition (CVD) in a horizontal tube furnace. After synthesis, the tubes were carefully purified by standard procedures to remove the catalyst [5]. Then, the partially purified product was treated with

A. Cortes (✉) · E. Svåsand · V. Lavayen · P. Häberle
Departamento de Física, Universidad Técnica Federico Santa
María, Valparaíso 2390123, Chile
e-mail: andrea.cortes@usm.cl

R. Segura
Departamento de Química y Bioquímica, Facultad de Ciencias,
Universidad de Valparaíso, Av. Gran Bretaña 1111,
Valparaíso, Chile

Fig. 1 Electron micrographs of MWCNTs. **a** TEM image of purified nanotubes and **b** HR-TEM image showing details of a tube wall in a single nanotube



HCl (6 M, 50 mL, 24 h). Afterward, this mixture was filtered and then washed thoroughly with deionized water. Finally, the product was dried at 250 °C in an Ar stream. Electron microscopy images (Fig. 1) show that MWCNTs have an average diameter close of 30 nm [6].

Carbon cone soot (MWCNCs) was kindly provided by *n*-tech, Norway. The material was produced in Kvearner Carbon black and hydrogen process [7]. As shown in Fig. 2, the carbon cone material consists of polymorph carbon particles with the form of disks (70%), cones (20%)

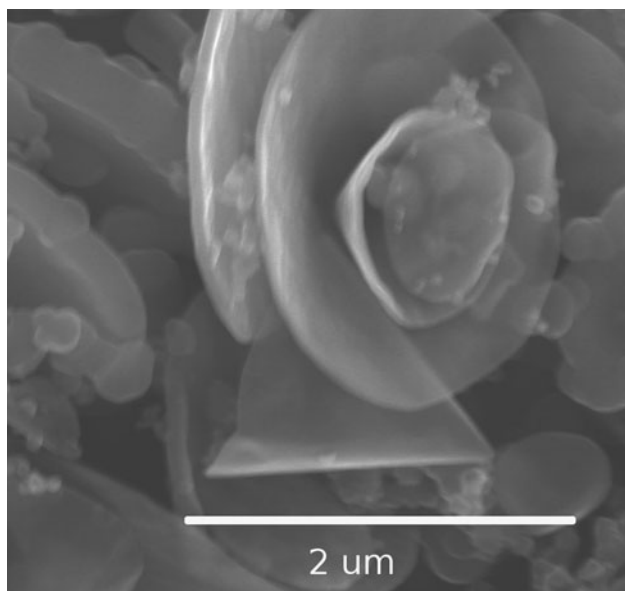


Fig. 2 SEM image of the carbon cone materials—as produced, showing the presence of carbon nanodisks. Some amorphous particles are observed on the surface of the cones

and some amorphous particles (10%). The five possible different cone angles are present in the sample. Most of the particles have a size in the range 0.5–3 μm, with the amorphous particles having characteristic sizes of a couple of hundreds of nanometers. The material was annealed at 2700 °C in an inert atmosphere for 3 h to increase the degree of graphitization.

Thin film preparation

Nanoheterostructure (NHS) films were obtained as follows: the carbonaceous product was dispersed in 2-propanol by the use of an ultrasonic bath. A spray paint technique was used to deposit the MWCNTs or MWCNC on FTO-glass. Next, a thin film of CdS was deposited on top of the carbon layer, using chemical bath deposition (CBD). The bath used for the deposition had a mixture of 0.06 M cadmium sulfate and 1.74 M ammonia. The mixture was kept at a constant temperature (75 °C) during treatment. Prethermalized thiourea (0.12 M) was added to the mixture, to induce the formation of CdS. NH₃ acts as a complexing agent during this process, whereas the thiourea provides sulfur [8].

Characterization

The microstructural characterization was carried out by scanning electron microscopy (JEOL JSM 840) equipped with electron dispersive spectroscopy (EDS). FEI Tecnai G2 F20 S-Twin microscope, operated at 200 kV was used to take the HR-TEM images. Transmission spectra were obtained with an OLIS 14 F UV–Vis–NIR spectrometer.

Photocurrent measurements

The current–voltage curves of the different heterostructures were recorded using a potentiostat. The device was put in an electrolytic cell with a three electrode configuration: platinum (counter electrode), saturated Ag/AgCl (reference electrode), and the device as the work electrode. A transparent electrolyte (Na_2SO_3 0.1 M) was used during the measurements. The cell was illuminated using a 50-W halogen bulb, which was pulsed periodically to allow the verification of the off-current as a function of time.

Results and discussion

High-resolution images (Fig. 1) of the purified MWCNTs provide some details regarding the level of graphitization of the nanotubes. The average diameter was estimated to be close to 30 nm, in agreement with our previous results [6]. The use of an aerograph to deposit the carbon nanostructures on the FTO substrate resulted in a homogeneous distribution of the carbon particles, as confirmed by SEM (not shown). The CBD created a smooth film of CdS covering the carbonaceous particles. In a previous report [8], some of us have shown that as-grown films made with the CBD technique, can display clusters with a globular surface morphology. Parameters, such as grain size, crystallographic structure, texture, roughness, etc., may be explained as a function of the 3D nucleation, and growth mechanisms. These parameters may be controlled in an effort to obtain thin films with desirable properties. The mean size of individual agglomerated grains was found to be around 100–150 nm for the as-grown films, as determined previously by AFM [8]. Energy dispersive spectroscopy (EDS) of the CdS films (not shown) give an atomic ratio Cd:S close to 1:1 as expected. The measured thicknesses of the heterostructures were approximately 200 nm.

Optical properties and bandgap energy determination

UV–Vis absorption spectroscopy is frequently used to characterize semiconductor films. Due to a low scattering in solid films, the bandgap (E_g) can be extracted from the spectra when the thickness of the film is known [9]. Determination of the bandgap from powder samples can also be performed by this technique if the incident light is absorbed or scattered before reaching the back surface of the sample. A thickness of 1–3 mm is required [10]. A reduced value of E_g is usually attributed to the creation of allowed energy states in the bandgap, at the time of film preparation, while a higher E_g value is linked to a size dependence of the gap if the film is made up of small grains

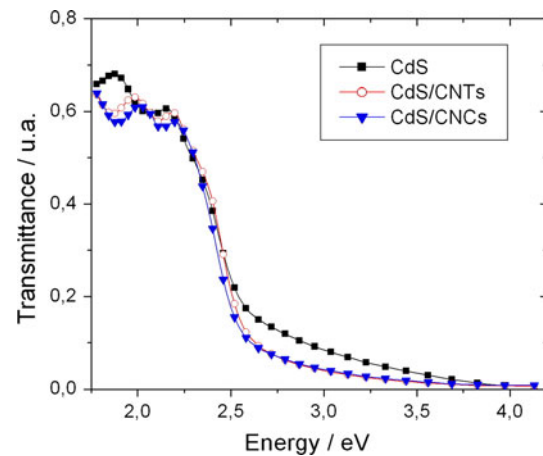


Fig. 3 Transmittance plot of heterostructures; **a** CdS/MWCNTs/FTO and **b** CdS/MWCNCs/FTO samples

[11]. Using the observed heterostructure film thickness as measured by electron microscopy, the bandgap was estimated to be 2.59 eV for both, the heterostructure film containing MWCNTs and the film with MWCNCs. This value is slightly higher than that of a pure CdS film, which has a bandgap of 2.56 eV. Figure 3 shows the UV–Vis spectra of the optical transmission of the CdS/MWCNTs/FTO and CdS/MWCNCs/FTO films. There is up to 55% transmission for wavelengths longer than 2.34 eV. A strong decrease in the transmission can be observed near the fundamental absorption band, as well as a shift to lower energies. The shift (indicated by the arrow direction in Fig. 3) is related to the crystallinity and thicknesses of the heterostructure films. A similar behavior was reported by Kityk et al. also in CdS [10]. Another interpretation of the observed shift is that quantum confinement begins to play a substantial role in the optical behavior of the film [10].

The UV–Vis spectra of the CdS/carbonaceous/FTO system does not show the first excitonic state of CdS nanoparticles (3.11 eV) neither the effects of a wide distribution in the particle size as seen in colloidal dispersions (4.90 eV). The observed behavior is indeed expected for a thin film of CdS. Several small peaks can be detected below 2.34 eV. They could be related to interference effects in light transmitted through the film and the substrate [12]. Similar behavior has been reported in the literature for CdS transmission spectra of films prepared by other techniques [13].

Photocurrent measurements

Illumination can create electron–hole pairs in semiconductor materials. However, electronic transfer to the electrodes (band-to-band electronic transitions) is hampered by the competing electron–hole recombination process, which

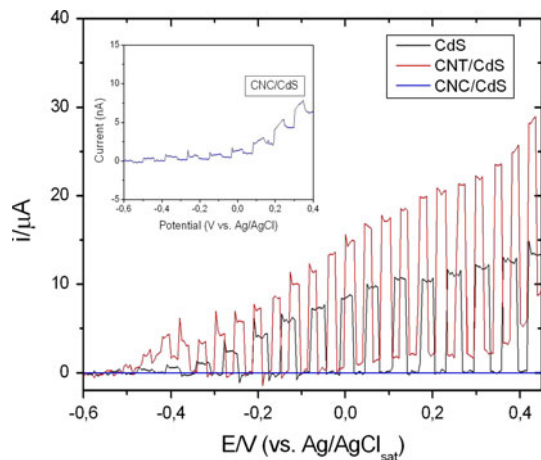


Fig. 4 Photocurrent under pulsed illumination of pure and modified CdS films. The periodic oscillation in the current is related to the on–off cycle of the light source. *Upper curve*: MWCNTs/CdS/FTO, *lower curve*; pure CdS and inset, in a much smaller scale, MWCNCs/CdS/FTO. The *solid blue line* in the main graph, which looks as a baseline, is indeed the MWCNCs/CdS/FTO current response

decreases the number of photogenerated carriers, hence diminishing the effective photocurrent. Therefore, to enhance the number of free carriers and the photocurrent, the retardation of the recombination process is essential. Figure 4 shows the I–V curves of the different heterostructure thin films, while the device was irradiated by a pulsed light source. A photocurrent was observed under these conditions. From the same figure, it is evident the CdS thin films, modified with MWCNTs, show a significant increase in the photocurrent with respect to the same structure formed only by CdS. The opposite effect is produced by the presence of MWCNCs and the photocurrent is strongly suppressed in the latter case.

All recording electrodes show photocurrent fluctuations immediately after the light is turned on. The current increases sharply followed by a small decay. Low-amplitude fluctuations in the current occur until the electrode is no longer illuminated and the total current decreases. This effect can be associated to recombination processes in shallow or bulk electrode defects [14, 15]. The illumination time dependence is not in the aim of the present report and will be described in more detail elsewhere.

The radical difference in the measured photocurrent in the two cases: (a) with MWCNTs and (b) with MWCNC is attributed to the chemical environment effect (oxygen groups), and/or the presence of defects. As the MWCNTs were acid treated, they are rich in defect sites and oxygen-based functional groups. These sites on the CNTs enable weak interactions between CdS and the carbon structures [2]. In the case of the carbon cone material no acid treatment was carried out, thus there is a minimal interaction between CdS and the cones. Hence, in this case the carbon

structures behave more like an insulating layer, decreasing the photocurrent output while in the case of MWCNTs the effect of acid treatment leads to an increment in the charge transfer capabilities of the heterostructure. As a result the role of these carbon nanostructures (MWCNTs) is to decrease the charge-transfer resistance in the system. Absorption spectroscopy results from a hetero-SWCNTs/CdS colloidal system suggests the existence of a strong excited-state interaction between CdS and the tubes, which results in a total quenching of the emission from CdS when SWCNTs are present together with the colloids [3]. Consistent with this observation a deactivation of excited CdS states by electron transfer to the CNTs seems reasonable. It should be pointed out that CNTs *alone* may be photoactive, but with a very low efficiency due to their ultrafast recombination of charge carriers [16]. Future efforts are needed to clarify this point.

Robel et al. [3] found that the photocurrent production in their CdS/SWCNTs system occurs by a two steps process. The main one consists of charge transfer from CdS to SWCNTs followed by charge transport to FTO and regeneration of the CdS by a redox couple. This last process is indeed a very slow one. Evidence of this two-step process has not been observed here, probably due to the reduced time resolution of our experiments. Ovits et al. [17] have prepared gold electrodes based on aniline modified with CdS nanoparticles (CdS NPs) functionalized further with SWCNTs. About 30–55% of the electrodes surface was covered by the nanocomposite. Photocurrent values of the aniline CdS-NP-CNTs composite were found to be higher than for the system without CNTs. CdS NP-CNTs composites, in this case, are crosslinked by bis-aniline redox-active bridging units. The result is an active matrix with a higher efficiency for generating a photocurrent. The high-photocurrent values generated in presence of SWCNTs have been attributed to the charge-transport properties of the tubes. Trapping of the photoexcited conduction band electrons retards their recombination. The effective removal of the electrons to the bulk electrode leads in principle to an increased efficiency in the generation of photo excited carriers.

As bottom line, the presence of SWCNTs in the composite allows the formation of bridges due to presence of aniline. As a result there is an improvement in charge separation, which in turn increases the photocurrent. In our devices, the MWCNTs are dispersed over FTO with the additional deposition of a homogenous layer of CdS. The enhancement in the photocurrent current in our case should be due to the presence of shallow (structural, optical) defects in the tube walls decorated by oxygen-based chemical groups, which in turn improve the charge transfer efficiency from the semiconductor.

Conclusion

A heterostructure consisting of carbon nanostructures and CdS on a FTO substrate is presented. The carbon nanostructures were deposited directly onto the conductive FTO electrode, by the use of aerograph, while the CdS was deposited using a chemical bath. Our experimental results for the CdS thin films, modified with MWCNTs, show a significant increase in the photocurrent with respect to the same structure using only CdS. These results are consistent with a higher efficiency either in charge collection or charged pair production. The acid treatment of the MWCNTs enhances the interactions between CdS and the oxygen-based functional groups and defect sites. We believe these “defects” increase the efficiency of the charge-transfer process. These findings are in accordance with the observed reduction of photocurrent in the CdS/MWCNTs/FTO, where the carbon cone material was used without acid treatment. The lack of defect sites and functional groups hinders the coupling between the CdS and carbon cone material, therefore making the electron transfer from CdS to the electrode more difficult. The use of acid-treated MWCNTs in CdS structures will be investigated in the future.

Acknowledgements This research was possible thanks to the financial support of the following grants: PBCT: PSD031 and ACT027, Fondecyt 3080058, 3090042, 1090683, 1090282, 11080232, MECESUP UVA0604 and Frinat 191579 (Norway). The authors thank P. Ulloa for the transmittance measurements; N-tech,

Norway, have kindly provided Carbon cones and other materials, and the Electrochemistry Laboratory at PUCV, Chile.

References

1. Kittel C (2005) Introduction to solid state physics, 8th edn. Wiley, USA, pp 1–680
2. Ichia S-H, Basnar B, Willner I (2005) *Angew Chem* 117:80
3. Robel BB, Kamat P (2005) *Adv Mater* 17:2458
4. Jeong SY, Lim SC, Bae DJ, Lee YH, Shin HJ, Yoon S, Choi JY, Cha OkH, Jeong MS, Perello D, Yun M (2008) *Appl Phys* 92:243103
5. Balasubramanian K, Burghard M (2005) *Small* 1:180
6. Segura RA, Tello A, Cárdenas G, Häberle P (2007) *Physica Status Solidi (a)* 204:513
7. Kvaerner ASA (1998) For production micro domain particles by use of a plasma process, Patent no. PCT/NO98/00093
8. Cortes HG, Marotti RE, Riveros G, Dalchiele EA (2004) *Sol Energy Mater Sol Cell* 82:21
9. Sahay PP, Nath RK, Tewari S (2007) *Cryst Res Technol* 42(3):275
10. Kityk V, Makowska-Janusik M, Ebothe J, El Hichou A, El Idrissi B, Addou M (2002) *Appl Surf Sci* 202:24
11. Popescu V, Pica EM, Pop I, Grecu R (1999) *Thin Solid Films* 349:67
12. Ni Y, Hao H, Cao X, Su S, Zhang Y, Wei X (2006) *J Phys Chem B* 110:17347
13. Moon B, Lee J, Jung H (2006) *Thin Solid Films* 511–512:299
14. Salvador P (1985) *J Phys Chem* 89:3863
15. Paul GS, Agarwal P (2009) *J Appl Phys* 106:103705
16. Guldi DM, Rahman GMA, Jux N, Tagmatarchis N, Prato M (2004) *Angew Chem Int Ed* 43(41):5526
17. Ovits O, Tel-Vered R, Baravik I, Wilner OI, Willner I (2009) *J Mater Chem* 19:7650